The N terminus of the small heat shock protein HSPB7 drives its polyQ aggregation-suppressing activity

Wu, Di; Vonk, Jan J; Salles, Felix; Vonk, Danara; Haslbeck, Martin; Melki, Ronald; Bergink, Steven; Kampinga, Harm H

Published in:
The Journal of Biological Chemistry

DOI:
10.1074/jbc.RA118.007117

Publication date:
2019

The N terminus of the small heat shock protein HSPB7 drives its polyQ aggregation–suppressing activity

Di Wu[1, 2], Jan J. Vonk[1], Felix Salles[1], Danara Vonk[1], Martin Haslbeck[3], Ronald Melki[4], Steven Bergink[1], Harm H. Kampinga[1]*

From the [1] University Medical Center Groningen, University of Groningen, Department of Biomedical Sciences of Cells and Systems, Antonius Deusinglaan 1, 9713 AV, Groningen, The Netherlands.
[2] College of Veterinary Medicine, Nanjing Agricultural University, Nanjing 210095, China
[3]Technische Universität München, Department Chemie, Lichtenbergstrasse 4, 85748 Garching, Germany
[4]Institut Francois Jacob (MIRCen), CEA and Laboratory of Neurodegenerative Diseases, CNRS 92265 Fontenay-Aux-Roses cedex, France

Running title: Role of NTD in HSPB7-function

*To whom correspondence should be addressed: Prof. Dr. Harm H. Kampinga: University Medical Center Groningen, University of Groningen, Department of Biomedical Sciences of Cells and Systems, Antonius Deusinglaan 1, 9713 AV, Groningen, Netherlands; email: h.h.kampinga@umcg.nl

Key words: heat shock protein family B (small) member 7 (HSPB7), polyglutamine aggregation, N-terminus, HSPB1, oligomerization, protein chaperone, intrinsically disordered region, CAG triplet expansion

ABSTRACT

Heat shock protein family B (small) member 7 (HSPB7) is a unique, relatively unexplored member within the family of human small heat shock proteins (HSPBs). Unlike most HSPB family members, HSPB7 does not oligomerize and so far has not been shown to associate with any other member of the HSPB family. Intriguingly, it was found to be the most potent member within the HSPB family to prevent aggregation of proteins with expanded polyglutamine (polyQ) stretches. How HSPB7 suppresses polyQ aggregation has remained elusive so far. Here, using several experimental strategies, including *in vitro* aggregation assays and immunoblotting and –fluorescence approaches, we show that the polyQ aggregation–inhibiting activity of HSPB7 is fully dependent on its flexible N-terminal domain (NTD). We observed that the NTD of HSPB7 is both required for association with and inhibition of polyQ aggregation. Remarkably, replacing the NTD of HSPB1, which itself cannot suppress polyQ aggregation, with the NTD of HSPB7 resulted in a hybrid protein that gained anti-polyQ aggregation activity. The hybrid NTD_{HSPB7}-HSPB1 protein displayed a reduction in oligomer size and, unlike wildtype HSPB1, associated with polyQ. However, experiments with phospho-mimicking HSPB1 mutants revealed that de-oligomerization of HSPB1 alone does not suffice to gain polyQ aggregation–inhibiting activity. Together, our results reveal that the NTD of HSPB7 is both necessary and sufficient to bind to and suppress the aggregation of polyQ-containing proteins.

Small heat shock proteins (HSPBs) are described as a series of small molecular size chaperones composed of a flexible N-terminal domain (NTD) and a flexible C-terminal domain (CTD) flanking a conserved α-crystallin domain (ACD) (1-3). The human family of HSPBs is comprised of 10 members (1). Most of these form highly dynamic oligomeric complexes (3,4). Besides forming homo-oligomeric complexes, some HSPBs can also form hetero-oligomers with specific other HSPBs (4,5). Exceptions to this paradigm are HSPB8, which forms a chaperone complex with BAG3 and Hsp70 (6,7), and HSPB7 which has no known other chaperone partners and does not form large oligomers (7,8).

Unlike the human oligomeric HSPB family members, HSPB7 overexpression does not enhance the cellular capacity to refold heat-unfolded luciferase (8) nor leads to suppression of the heat-inducd aggregation of cytosolic proteins (9). Instead, within the human HSPB family, HSPB7 is the strongest suppressor of aggregation of polyglutamine containing proteins (8) that cause diseases like Spinocerebellar Ataxia's, Kennedy's disease, and Huntington's disease (HD) (10,11). These diseases are caused by expansions of CAG triplet repeats coding for abnormally long polyglutamine (polyQ) stretches (11). The size of these expansions are inversely correlated with the onset age of these diseases and to the aggregation propensity of the respective proteins (10). Unlike heat-induced aggregates that are generally driven by hydrophobic interactions (12), polyQ aggregation is suggested to be driven by hydrogen bonding and beta-hairpin structures (13,14) potentially explaining the different dependence on chaperone activity for suppression of

polyQ aggregation. However, why HSPB7 stands out as most potent suppressor of polyQ aggregation within the HSPB family, has remained an enigma. Previously, we showed that HSPB7 requires (macro) autophagy for its suppressive action on polyQ aggregation (8). However, HSPB7 differs from other autophagy related suppressors like Alfy, as it cannot act on preformed aggregates to fullfill its function (15). One model that explains this finding predicts that HSPB7 is present during aggregate formation and binds these protofibrils to maintain early aggregates in a state competent for processing by the autophagic machinery (16).

In this manuscript, we investigated which characteristics of HSPB7 are required to chaperone polyQ proteins and prevent their aggregation. HSPB7 acts directly on the aggregation process as recombinant HSPB7 can delay *in vitro* polyQ aggregation, whereas HSPB1 cannot. HSPB7 acts mainly on regions flanking the polyQ and not on the amyloid core itself. In cells, this remarkable suppression depends on the N-terminus of HSPB7 that is predicted as an intrinsically disordered region. While the N-terminus by itself is not capable of supressing aggregation, fusion to the alpha crystallin domain of HSPB1 results in a hybrid protein with polyQ anti aggregation properties. In summary, the full and unique N-terminal domain is key to the specific ability of HSPB7 to inhibit polyQ aggregation.

Results

The full NTD is required for HSPB7 to prevent polyQ aggregation

Within the HSPB family, cell-based analyses had revealed that HSPB7 stands out as a chaperone that is the most capable to prevent aggregate formation by amyloidogenic polypeptides including polyglutamine (polyQ) containing proteins (8). First, we asked whether this protective function of HSPB7 against polyQ aggregation seen in cells is related to a direct action of the chaperone on the substrate. Hereto, we incubated a purified exon-1 fragment of mutant Huntingtin with 48 glutamines (mHttQ48) with either purified HSPB7 or HSPB1 (with HSPB1 acting as control as it is unable unable to protect against polyQ aggregation in cells (8)). Analysing the ratio of soluble:insoluble mHttQ48 by gel-electrophoresis (9), we found that with time, the amount of soluble mHttQ48 declined and appeared as aggregated material in the stacking gel (Figure 1, A, B). The rate of decline in the soluble:insoluble ratio of mHttQ48 was unaffected by co-incubation with HSPB1 but clearly slowed down by the presence of HSPB7 (Figure 1, A, B) meaning that HSPB7 acts directly on the aggregation process.

Next, we asked what structural characteristics in HSPB7 specifies this activity towards suppressing aggregation of polyQ proteins. The NTDs and CTDs of HSPBs display the highest level of variability and have been suggested to be crucial for their differential function (17,18). Our earlier data had revealed that the CTD of HSPB7 is not required for its activity to prevent polyQ aggregation (8). So, we focused our attention on the NTD of HSPB7 and noted a serine-rich stretch (SRS) (Figure 1, C and Supporting Information 1, A) that is not found in other HSPB members. Interestingly, a serine-rich stretch has been identified as a crucial segment in the ability of DNAJB6, a Hsp70 co-chaperone, to suppress polyQ aggregation (19,20). Although structurally distinct (Supporting Information 1, A) we first set out to test the importance of the NTD in HSPB7, and in particular its SRS, in its action to supress polyQ aggregation by generating a series of NTD truncations of HSPB7 mutants (Figure 1, C) that we co-expressed in cells together with a exon-1 fragment of Huntingtin with 74 glutamines tagged to GFP (mHttQ74-GFP). In contrast to our speculations, deleting the SRS from HSPB7 (v5-HSPB7$^{\Delta S17\text{-}29}$) did not result in a loss of its anti-aggregation activity (Figure 1, D-F), despite its relatively lower expression as compared to that of wildtype HSPB7 (Supporting Information 1, B). However, a gradual decline in anti-aggregation activity was found upon progressive NTD deletion with the complete deletion of the NTD (v5-HSPB7$^{\Delta 73}$), being inactive (Figure 1, D-F, Supporting Information 1, B). None of the HSPB7 variants caused an induction of the heat shock response, evidenced by the absence of induced expression of HSPA6, an exclusive HSF-1 regulated chaperone (21,22) (Supporting Information 1, C). Also the HSF-1 regulated chaperone DNAJB1, that -when overexpressed alone- can also lead to suppression of polyQ aggregation in these cells (23,24) was not elevated by the expression of any of the HSPB7 variants (Supporting Information 1, C), implying that it is unlikely that their (remaining) protective effects are due to upregulation of endogeneous stress responses. Finally, endogenous expression of HSPB7 is undetetcable in these cells irrespective of expression of the HSPB7 variants (not shown) implying that protective effects of the mutants cannot be attributed to formation of complexes between full length endogenous and the ectopically expressed HSPB7 variants.

Fusing the NTD of HSPB7 to polyQ does not prevent polyQ aggrgation

Three algorithms designed to predict intrinsically disordered regions (25,26) suggest that the NTD of HSB7 is highly disordered (Supporting Information 1, D) and reminiscent of proteins involved in phase separation (27-29) In fact, HSPB7 has been shown to be associated with intranuclear RNA speckles (SC35 speckles) and the fusion of its NTD to other small HSPBs like HSPB1 (of which the NTD is

less disordered: Supporting Information 1, D and E) suffices to drive their association with these SC35 speckles, suggesting it might induce phase separation of the proteins it interacts with to prevent amyloidogenesis (30). Whereas for polyQ proteins, a protective role for chaperone-mediated phase separation has not been established, it has been speculated that in yeast compartmentalization of polyQ proteins into so-called insoluble protein deposit (iPODs) may have physiological, cell protective relevance (31,32). In HEK293 cells, wild type HSPB7 (v5-HSPB7^{WT}) indeed colocalizes with mHttQ74-GFP inclusions and this co-localization is much reduced for the NTD deletion mutant (v5-HSPB7$^{\Delta 73}$) (Figure 1, G). Moreover, whereas full length HSPB7 was bound to mHttQ74-GFP in co-immunoprecipitation experiments the NTD deletion mutant (v5-HSPB7$^{\Delta 73}$) was not (Figure 1, H). This could suggest that binding of HSPB7 to polyQ proteins drives its phase separation and hence prevents its aggregation into SDS-insoluble amyloids. Our initial-attempts to co-express mHttQ74-GFP with only the NTD of HSPB7 (NTD$_{HSPB7}$) failed as the NTD alone is not stable when expressed in cells (Supporting Information 2, A). To test whether the predicted major IDR fragment of HSPB7 suffices to prevent polyQ aggregation, we therefore tagged the polyQ fragment directly with the NTD of HSPB7 (Figure 2, A-D, Supporting Information 2, B). However, for both fragments with either 43 or 74 CAG repeats, tagging with the NTD$_{HSPB7}$ did not prevent polyQ aggregation, but rather enhanced it. (Figure 2, A-D). These data imply binding of HSPB7 to polyQ proteins and a putative subsequent phase separation driven by its NTD as such is insufficient to prevent polyQ aggregation. Direct fusion of the full length HSPB7 to polyQ74 did prevent aggregation indicating that the NTD in these hybrid fusion proteins is functional (Figure 2, E and F, Supporting Information 2, C). Since we previously showed that the CTD of HSPB7 is dispensable for its action on polyQ (8), the combined data suggest that interaction of a (monomeric) HSPB7 via its NTD to polyQ proteins and the presence of the ACD of HSPB7 suffice to prevent mHtt aggregation.

Fusion of the NTD of HSPB7 to HSPB1 is sufficient to convey HSPB1 with anti-polyQ aggregation activity

We next hypothesized that fusing the NTD of HSPB7 to the ACD of other HSPBs may turn these into polyQ aggregation preventive chaperones. As mentioned above, HSPB7 does not form homo- nor hetero-oligomers with any of the HSPBs, so targeting the other HSPBs to polyQ aggregates via hetero-oligomerisation is unlikely to occur. To test whether the NTD of HSPB7 could turn another HSPB protein into an effective inhibitor of polyQ aggregation we choose HSPB1, as neither its presence in vitro (Figure 1, A-B) nor its overexpression in cells (Figure 3, B-D, Supporting Information 3, A) could inhibit polyQ aggregation. Strikingly, expression of a fusion of the NTD of HSPB7 with the ACD and C-terminal domain of HSPB1 (NTD$_{HSPB7}$-HSPB1) lead to reduced mHttQ74-GFP aggregation comparable to the effect of HSPB7^{WT} expression (Figure 3, A-D). This result indicated that the conserved ACD is a necessary structural requirement for HSPB7 to prevent polyQ aggregation. Strikingly, this requirement is not restricted to the ACD of HSPB7 as also the ACD of HSPB1 can exert this function. Indeed, a fusion of the NTD$_{HSPB7}$ to mRFP (as a control) did not generate a hybrid protein that could prevent mHttQ74 aggregation (Supporting Information 3, B and C).

In line with the biochemical data, we found that whereas wild type HSPB1 did not co-localize with mHttQ74-GFP, the NTD$_{HSPB7}$-HSPB1 hybrid did (Figure 3, E). Inversely, replacing the NTD of HSPB7 with the NTD of HSPB1 resulted in a hybrid protein (NTD$_{HSPB1}$-HSPB7) that had lost its anti-polyQ-aggregation activity (Figure 3, F and G, Supporting Information 3, D) and no longer co-localized with the polyQ aggregates (Figure 3, H).

The co-localization of polyQ with HSPB7 and NTD$_{HSPB7}$-HSPB1 suggested that the NTD of HSPB7 is both required and sufficient for association of small HSPB proteins with polyQ proteins. This was confirmed by GFP pull-down experiments with mHttQ74-GFP. Whereas HSPB7^{WT} was clearly co-precipitating with mHttQ74-GFP, HSPB7$^{\Delta 73}$ did not (Figure 1, H). Inversely, whereas HSPB1^{WT} did not co-IP with mHttQ74-GFP, NTD$_{HSPB7}$-HSPB1 did (Figure 3, I). These data confirm that the NTD of HSPB7 drives the interaction between HSPB7 and polyQ proteins. Since the interaction in our co-IP experiments is performed on soluble material, these data further suggest that the N-terminus of HSPB7 can already bind to polyQ prior to its insolubilization into high molecular weight aggregates. This mode of action is analogous to those of other small HSPs that need to be present prior to aggregation to be most active as well (7,33). Our data suggest that the flanking regions, here the NTD, are required and sufficient for targeting small HSPs to their substrates and that the ACD enables the suppression of aggregation.

Shifting the HSPB oligomeric status is not sufficient for polyQ aggregation prevention

How can the NTD of HSPB7 turn HSPB1 into a protein that now can bind to polyQ proteins and suppress their aggregation? Since, HSPB7 does not form oligomers like the canonical small HSPs including HSPB1 (8), we determined the role of the HSPB7-NTD in the oligomerization process. Sucrose gradient centrifugation of whole cell extracts confirmed that wild type HSPB1 is polydispersed (Figure 4, A), reminiscent of being present as dynamic

oligomers in cells. In contrast, wild type HSPB7 predominantly runs in a monodispersed peak, likely representing dimers. (Figure 4, A). Deletion of the NTD from HSPB7 (HSPB7$^{\Delta 73}$) does not change this behavior (Figure 4, A) , implying that loss of its anti-aggregation activity is not related to a change into a more polydispersed form. Importantly, fusion of the HSPB7-NTD to HSPB1 (NTD$_{HSPB7}$-HSPB1) has a strong impact on the oligomeric properties of HSPB1. The NTD$_{HSPB7}$-HSPB1 chimera was found to sediment in the same fractions as HSPB7, representing smaller oligomeric species such as dimers (Figure 4, A). These data indicate that the presence of the HSPB7-NTD inhibits the association of the HSPB to higher oligomeric asslemblies and might point to an association between the oligomeric status of HSPBs and their ability to prevent polyQ aggregation.

To test whether the shift in oligomerization behavior suffices to turn HSPB1 into a polyQ aggregation preventing chaperone, we used HSPB1-phosphorylation mutants that also impede the oligomeric status. HSPB1 can be phosphorylated at three serines which drives its de-oligomerization (34,35). Mutation of these three serines (S) into aspartic acid (D) (HSPB1^{DDD}) simulates the oligomeric behavior of this phosphorylated form of HSPB1 (34) (Figure 4, B; Supporting Information 3, E), whilst mutating these serines into alanines (HSPB1^{AAA}) simulate the un-phosphorylated form of HSPB1 forming, on average, larger oligomeric complexes (34) (Figure 4, B; Supporting Information 3, F). However, expression of neither HSPB1^{DDD} nor HSPB1^{AAA} was found to reduce mHttQ74-GFP aggregation (Figure 4, C, Supporting Information 3, F). These results suggest that de-oligomerization alone is not sufficient for HSPB1 to prevent polyQ aggregation and pinpoints the need for the presence of the HspB7-NTD for polyQ protein recognition.

The ability of HSPB7 to prevent polyQ aggregation depends on the regions flanking the polyQ stretch.

The polyQ stretch in (mutant) huntingtin is flanked by a 17 amino acid long N-terminal (N17) domain (36) and a proline-rich region (PRR) C-terminal (37) of the poly-Q stretch. These flanking regions not only affect the propensity of aggregation of the polyQ protein, but also affect how chaperones may or may not be able to delay the onset of aggregation (10,36,37). Whereas some chaperones like DNAJB6 can prevent initiation of aggregation independently of such flanking regions by directly interacting with the amyloidogenic polyQ region (10), other chaperones like TRiC mediate their anti-aggregation effects via binding to the N17 domain of Huntingtin (10,38). To test how HSPB7 acts, we co-expressed it with 4 different mHtt constructs (Figure 5, A-D) one containing both the intact N17 domain and PRR, one with a truncated N17, one with a truncated PRR, or one in which both the N17 and PPR are truncated. HSPB7 could suppress the aggregation of all these variants, except the one with a truncation of both the N17 domain and the PPR constructs (Figure 5, A-D). This implies that HSPB7 does not directly act on the amyloidogenic polyQ region but requires either the N17 domain and/or the PPR to mediate its anti-aggregation effects.

Discussion

Here we show that HSPB7, a non-canonical member of the human HSPB family of small heat shock proteins, prevents aggregate formation by directly acting on polyglutamine (polyQ) containing proteins via its unique N-terminal domain. This NTD facilitates binding of HSPB7 to polyQ proteins. Intriguingly, the NTD is sufficient to provide another member of the HSPB family, HSPB1, with the capacity to bind to and suppress aggregation of polyQ proteins.

HSPB7, unlike canonical HSPBs, is not forming large oligomeric species (8). Although replacing the NTD of HSPB1 by the NTD of HSPB7 leads to a reduction in the average oligomeric size of the hybrid protein, de-oligomerization alone was found insufficient to confer anti-polyQ aggregation activity to HSPB1. Rather, the NTD of HSPB7 seems to confer substrate binding capacity to HSPBs as its deletion from HSPB7 (HSPB7$^{\Delta 73}$) lead to a loss of binding and suppression capacity. Currently it is unclear to which polyQ species HSPB7 is binding. Our co-IP experiments, perfomed using soluble material, suggest that HSPB7 binds to early profibrillar species. The fact that HSPB7 is associated with the (later) polyQ inclusions (IF) confirms its capacity to bind to polyQ species, but may also reflect a failed function.

Interestingly, the NTD of HSPB7 is intrinsically disordered (27), characteristic of proteins involved in phase separation (39,40). Although we did not observe any HSPB7-mediated demixing, our results do not rule out a role of the NTD in phase separation. The unique properties of the NTD of HSPB7 in the context of an ACD are clearly sufficient to drive inhibition of polyQ aggregation. The notion that this suppressive nature gradually declines with the progressive shortening of the NTD (Figure 1) is arguing against the presence of specific structural motifs within the NTD. Indeed for other intrinsically disordered regions, it has been shown that rather than amino acid order and chemical composition, function is determined by the length of the IDR (40). These results further underscore the possible IDR-like characteristics of the NTD of HSPB7 being crucial for its anti-amyloidogenic activity. Yet, these features alone do not suffice to confer such activity as fusion of the NTD of HSPB7 to polyQ proteins directly did not reduce but rather enhanced polyQ aggregation (Figure 2, A-D).

Our combined data suggest that the NTD of HSPB7 drives a de-oligomerization of HSPB proteins that causes exposure of its IDR-like features that next drives binding of the HSPB to early intermediate aggregates of polyQ proteins, by interacting with regions flanking the amyloidogenic polyQ core. Through such interactions further oligomerization into amyloid like fibers is delayed (41). Alternatively early formed protofibrils are stabilized by HSPB7 to inhibit the rate of the aggregation process (41,42). Irrespective of either one of these mechnisms, aggregate growth is delayed which may facilitate their engulfment into autophagosomes to facilitate aggrephagy (8,15,16).

Experimental procedures

Cell culture and transient transfection

HEK293 cells were grown in DMEM (GBICO) containing 10% FCS (Greiner Bio-one), 100 Units/ml Penicillin/streptomycin (Invitrogen). For transient transfection, 3.5×10^5 cells were seeded on poly-lysine (Sigma) pre-coated 6-well plates or cover slips. Cells were cultured until about 70% confluency and were transfected with polyethylenimine (PEI) (Invitrogen) following the manufacturer's protocol.

In vitro aggregation of mHtt

Purified HSPB1 and HSPB7 (9) and a mHttQ48 exon-1 fragment containing the N17 domain, 48 glutamines and the PPR protein (43) were used for *in vitro* aggregate formation (9). In short, 20 µM mHttQ48 was incubated with 20 µM sHSPB at 37 ℃ for 0, 1, 2, 3, 4 and 5 hours in PBS (pH=7.4) containing 1 mM DTT. After incubation, 8 µl of each sample was mixed with the same amount of denaturing buffer (180 mM Tris-HCl, pH 6.8, 30% glycerol, 15% beta-mercaptoethanol, 6% SDS) (43) and then immediately be boiled in 95 ℃ for 5 min. Samples were stored at -140℃ until use. Samples were boiled before loading onto a 12% SDS-PAGE gel. After electrophoresis, the gel was stained by SYPRO Orange (Sigma). Images were analysed using a ChemiDoc Touch Imaging system (Bio-Rad). Hereafter, the gel was washed in washing buffer (25 mM Tris base, 190 mM glycine and 0.1% SDS, pH=8.3) for three times, followed by transfer onto a nitrocellular membrane for regular western blot analyses.

Gene cloning and generation of mutants

Construction of v5-HSPB7^{WT}, v5-HSPB7$^{\Delta s17\text{-}29}$, NTD$_{HSPB7}$-mRFP and mHttQ74-GFP plasmid has been described before (8). v5-HSPB7$^{\Delta 16}$, v5-HSPB7$^{\Delta 31}$, v5-HSPB7$^{\Delta 73}$, N10-Q74-PRR, N17-Q74-P10 and N10-Q74-P10 were generated using QuickChang XL Site-Directed Mutagenesis Kit (Agilent Technologies) with v5-HSPB7^{WT} or N17-Q74-PRR (mHttQ74 full exon1) as templates, all steps followed the instructions of manufacturer. To generate v5-NTD$_{HSPB7}$Q43-eGFP, v5-NTD$_{HSPB7}$Q74-eGFP, and v5-HSPB7^{WT}-Q74-eGFP, v5-NTD$_{HSPB7}$ (the N-terminus of HSPB7 with a v5 tag) or v5-HSPB7^{WT} was cloned from v5-HSPB7^{WT} by PCR, adding unique BamHI and NheI sites to the 5' and 3' terminus respectively. GFP tagged polyQ fragments were obtained by cuting mHttQ43-GFP and mHttQ74-GFP plasmids using NheI and NotI. The inserts were ligated into the BamHI and NotI digested pcDNA3.1 vector. A similar strategy was used to generate v5-NTD$_{HSPB7}$HSPB1 but based on v5-HSPB7^{WT}, empty pcDNA3.1 vector and v5-HSPB1^{WT} plasimds (8). The HSPB1^{DDD} and HSPB1^{AAA} mutants have been reported before (34).

Primers.

Primer used for cloning the NTD of HSPB7: F: 5'-GCTACCGGATCCAGCCACAGAACCTCTTCCACCTTCCGAG-3'; R: 5'-CGTACGGCTAGCGCCTGCCCCACCGGGGCGGGCTGGGAA-3'. Primers used for cloning HspB7: F: 5'-GCTACCGGATCCAGCCACAGAACCTCTTCCACCTTCCGAG-3'; R: 5'-GCTACTGCTAGCGATTTTGATCTCCGTCCGGAAGGTC-3'.

Sucrose gradient centrifugation

Sucrose gradient analysis was done as reported before (8). Briefly, transfected HEK293 cells were washed with PBS and lysed in 200µl NP40 lysis buffer (50mM HEPES, 60mM KCl, 2mM MgCl2, 10% glycerol, 0.4% NP40). Cell lysates were cleared through a 26 gauge syringe for 10 times, followed by centrifugation at 100000g for 16 hours using 20%-60% sucrose gradient colum in a ultraspeed centrifuge using a SW41 rotor. 700µl fractions were precipitated by adding equal amount of 25% trichloroacatic acid. The pellets were washed twice using 80% acetone (-20℃) and allowed to dry. The pellet was dissolved in 20µl 0.1M NaOH containing 1% SDS. Equal amount of 2× Laemmli buffer was added and samples were boiled for 5 minutes before western blot analysis.

Immunoblotting

For western Blot, cells were lysed in FTA sample buffer (10mM Tris-HCl, 150mMNaCl, 2% SDS, pH=8.0) and were boiled with equal amount of 2× Laemmli buffer. Samples were then loaded and run on a 12% SDS page gel and transfered (Bio-Rad). After transfer, membranes were blocked and incubated with primary and secondary antibodies followed by detection using the ChemiDoc Touch Imaging system (Bio-Rad)

Filter trap assays (FTA) were perfomed as reported before (33). In short, 3.5×10^5 HEK293 cells were seeded on 6 well plates. Cells in each well were lysed in 200 µl FTA sample buffer (10 mM Tris-Cl, pH 8.0, 150 mM NaCl, 2% SDS). 100 µg, 20 µg and 4 µg samples were diluted in FTA sample buffer supplied with 50 mM dithiothreitol (DTT). Boiled samples were then applied onto a pre-washed (by FTA wash

buffer, 10 mM Tris-Cl, pH 8.0, 150 mM NaCl, 0.1% SDS) 0.2 µM cellulose acetate filter (GE Water and Process Technologies, Trevose, PA, USA) with 2 Whattman papers (Bio-Rad, Hercules, CA, USA) in a Bio-Dot microfiltration apparatus (Bio-Rad). Gentle suction was applied to filtrate the samples followed by three times washing using FTA wash buffer. After blocking the membrane for 1 h in 5% milk, incubated with primary (overnight) and secondary antibodies (1 h), membrane was exposed using ChemiDoc Touch Imaging system (Bio-Rad).

Primary and secondary antibodies used: mouse anti-v5 primary antibody (invitrogen) at a 1:10000 dilution, anti-GAPDH primary antibody (Fitzgerald) at 1:10000 dilution, anti-GFP primary antibody (invitrogen) at1:5000 dilution, anti-HSPB1 primary antibody (StressMarq) at 1:2000 dilution, anti-polyglutamine primary antibody (MAB1574, Sigma) at 1:1000 and sheep anti-mounse secondary anitbody (GE Healthcare life science) at 1:5000 dilution.

Immunofluorescence

48 hours after transfection, cells on coverslips were fixed in 2% formaldehyde for 15 min., washed 2 times with PBS (pH=7.5) and permeabilized with PBS-TritonX100 (0.1%). Then cells were washed with PBS and with PBS plus (PBS with 0.5% BSA, 0.15% glycine), followed by primary antibody incubation overnight at 4 ℃. Then cells on coverslips were washed with PBS plus for 4 times and were incubated with secondary antibody. After washing with PBS plus and PBS DNA was stained with DAPI (Thermo Fisher Scientific) for 5 minutes followed by washing with PBS. Cover slips were mounted in vectashield (Agar Scientific). Mouse anti-v5 primary antibody (invitrogen) at a 1:10000 dilution, Alexa 594 anti-mouse (Invitrogen) secondary antibody was diluted as 1:1500. Images were taken by a Leica sp8 confocal microscope and edited by Fiji.

Statistical analysis

The software Curve Expert 1.3 was used to make a standard curve for measuring protein concentration. Differences among the experimental groups were analyzed by one-way analysis of variance (ANOVA) ($P < 0.05$ and $P < 0.01$). Values were considered to differ significantly when $P < 0.05$. All data are expressed as the mean ± one standard deviation (SD). All experiemnts were repeated for at least three times.

Acknowledgments

This research is supported by China Scholarship Council (CSC: 201606850004) awarded to Di Wu, ZonMW - Top Grant (projectnummer 91217002: Harm Kampinga), the JPND project “Protest-70” (PATHWAYS-200-115: Ronald Melki and Harm H. Kampinga), and a grant from the DFG (SFB1035: Martin Haslbeck. We thank Evgeny Mymrikov and Constanze Kainz for technical assistance and Els Kuiper for generating the different polyglutamine constructs.

Conflicts of interests Statement.

The authors declare that they have no conflicts of interest with the contents of this article.

References

1. Garrido, C., Paul, C., Seigneuric, R., and Kampinga, H. H. (2012) The small heat shock proteins family: the long forgotten chaperones. *Int J Biochem Cell Biol* **44**, 1588-1592
2. Sun, Y., and MacRae, T. H. (2005) Small heat shock proteins: molecular structure and chaperone function. *Cell Mol Life Sci* **62**, 2460-2476
3. Haslbeck, M., Franzmann, T., Weinfurtner, D., and Buchner, J. (2005) Some like it hot: the structure and function of small heat-shock proteins. *Nat Struct Mol Biol* **12**, 842-846
4. Arrigo, A. P. (2013) Human small heat shock proteins: protein interactomes of homo- and hetero-oligomeric complexes: an update. *FEBS Lett* **587**, 1959-1969
5. Mymrikov, E. V., Seit-Nebi, A. S., and Gusev, N. B. (2012) Heterooligomeric complexes of human small heat shock proteins. *Cell Stress Chaperones* **17**, 157-169
6. Carra, S., Seguin, S. J., Lambert, H., and Landry, J. (2008) HspB8 chaperone activity toward poly(Q)-containing proteins depends on its association with Bag3, a stimulator of macroautophagy. *J Biol Chem* **283**, 1437-1444
7. Carra, S., Rusmini, P., Crippa, V., Giorgetti, E., Boncoraglio, A., Cristofani, R., Naujock, M., Meister, M., Minoia, M., Kampinga, H. H., and Poletti, A. (2013) Different anti-aggregation and pro-degradative functions of the members of the mammalian sHSP family in neurological disorders. *Philos Trans R Soc Lond B Biol Sci* **368**, 20110409
8. Vos, M. J., Zijlstra, M. P., Kanon, B., van Waarde-Verhagen, M. A., Brunt, E. R., Oosterveld-Hut, H. M., Carra, S., Sibon, O. C., and Kampinga, H. H. (2010) HSPB7 is the most potent polyQ aggregation suppressor within the HSPB family of molecular chaperones. *Hum Mol Genet* **19**, 4677-4693
9. Mymrikov, E. V., Daake, M., Richter, B., Haslbeck, M., and Buchner, J. (2017) The Chaperone Activity and Substrate Spectrum of Human Small Heat Shock Proteins. *J Biol Chem* **292**, 672-684
10. Kuiper, E. F., de Mattos, E. P., Jardim, L. B., Kampinga, H. H., and Bergink, S. (2017) Chaperones in Polyglutamine Aggregation: Beyond the Q-Stretch. *Front Neurosci* **11**, 145
11. Zoghbi, H. Y., and Orr, H. T. (2000) Glutamine repeats and neurodegeneration. *Annu Rev Neurosci* **23**, 217-247
12. Kim, Y. E., Hipp, M. S., Bracher, A., Hayer-Hartl, M., and Hartl, F. U. (2013) Molecular chaperone functions in protein folding and proteostasis. *Annu Rev Biochem* **82**, 323-355
13. Kar, K., Hoop, C. L., Drombosky, K. W., Baker, M. A., Kodali, R., Arduini, I., van der Wel, P. C., Horne, W. S., and Wetzel, R. (2013) beta-hairpin-mediated nucleation of polyglutamine amyloid formation. *J Mol Biol* **425**, 1183-1197
14. Kar, K., Baker, M. A., Lengyel, G. A., Hoop, C. L., Kodali, R., Byeon, I. J., Horne, W. S., van der Wel, P. C., and Wetzel, R. (2017) Backbone Engineering within a Latent beta-Hairpin Structure to Design Inhibitors of Polyglutamine Amyloid Formation. *J Mol Biol* **429**, 308-323
15. Eenjes, E., Dragich, J. M., Kampinga, H. H., and Yamamoto, A. (2016) Distinguishing aggregate formation and aggregate clearance using cell-based assays. *J Cell Sci* **129**, 1260-1270
16. Vos, M. J., Zijlstra, M. P., Carra, S., Sibon, O. C., and Kampinga, H. H. (2011) Small heat shock proteins, protein degradation and protein aggregation diseases. *Autophagy* **7**, 101-103
17. Carra, S., Alberti, S., Arrigo, P. A., Benesch, J. L., Benjamin, I. J., Boelens, W., Bartelt-Kirbach, B., Brundel, B., Buchner, J., Bukau, B., Carver, J. A., Ecroyd, H., Emanuelsson, C., Finet, S., Golenhofen, N., Goloubinoff, P., Gusev, N., Haslbeck, M., Hightower, L. E., Kampinga, H. H., Klevit, R. E., Liberek, K., McHaourab, H. S., McMenimen, K. A., Poletti, A., Quinlan, R., Strelkov, S. V., Toth, M. E., Vierling, E., and Tanguay, R. M. (2017) The growing world of small heat shock proteins: from structure to functions. *Cell Stress Chaperones* **22**, 601-611

18. van Montfort, R. L., Basha, E., Friedrich, K. L., Slingsby, C., and Vierling, E. (2001) Crystal structure and assembly of a eukaryotic small heat shock protein. *Nat Struct Biol* **8**, 1025-1030
19. Hageman, J., Rujano, M. A., van Waarde, M. A., Kakkar, V., Dirks, R. P., Govorukhina, N., Oosterveld-Hut, H. M., Lubsen, N. H., and Kampinga, H. H. (2010) A DNAJB chaperone subfamily with HDAC-dependent activities suppresses toxic protein aggregation. *Mol Cell* **37**, 355-369
20. Kakkar, V., Mansson, C., de Mattos, E. P., Bergink, S., van der Zwaag, M., van Waarde, M. A., Kloosterhuis, N. J., Melki, R., van Cruchten, R. T., Al-Karadaghi, S., Arosio, P., Dobson, C. M., Knowles, T. P., Bates, G. P., van Deursen, J. M., Linse, S., van de Sluis, B., Emanuelsson, C., and Kampinga, H. H. (2016) The S/T-Rich Motif in the DNAJB6 Chaperone Delays Polyglutamine Aggregation and the Onset of Disease in a Mouse Model. *Mol Cell*
21. Ramirez, V. P., Stamatis, M., Shmukler, A., and Aneskievich, B. J. (2015) Basal and stress-inducible expression of HSPA6 in human keratinocytes is regulated by negative and positive promoter regions. *Cell Stress Chaperones* **20**, 95-107
22. Mendillo, M. L., Santagata, S., Koeva, M., Bell, G. W., Hu, R., Tamimi, R. M., Fraenkel, E., Ince, T. A., Whitesell, L., and Lindquist, S. (2012) HSF1 drives a transcriptional program distinct from heat shock to support highly malignant human cancers. *Cell* **150**, 549-562
23. Heldens, L., van Genesen, S. T., Hanssen, L. L., Hageman, J., Kampinga, H. H., and Lubsen, N. H. (2012) Protein refolding in peroxisomes is dependent upon an HSF1-regulated function. *Cell Stress Chaperones* **17**, 603-613
24. Rujano, M. A., Kampinga, H. H., and Salomons, F. A. (2007) Modulation of polyglutamine inclusion formation by the Hsp70 chaperone machine. *Exp Cell Res* **313**, 3568-3578
25. Kozlowski, L. P., and Bujnicki, J. M. (2012) MetaDisorder: a meta-server for the prediction of intrinsic disorder in proteins. *BMC Bioinformatics* **13**, 111
26. Meszaros, B., Erdos, G., and Dosztanyi, Z. (2018) IUPred2A: context-dependent prediction of protein disorder as a function of redox state and protein binding. *Nucleic Acids Res* **46**, W329-W337
27. Sudnitsyna, M. V., Mymrikov, E. V., Seit-Nebi, A. S., and Gusev, N. B. (2012) The role of intrinsically disordered regions in the structure and functioning of small heat shock proteins. *Curr Protein Pept Sci* **13**, 76-85
28. Morelli, F. F., Verbeek, D. S., Bertacchini, J., Vinet, J., Mediani, L., Marmiroli, S., Cenacchi, G., Nasi, M., De Biasi, S., Brunsting, J. F., Lammerding, J., Pegoraro, E., Angelini, C., Tupler, R., Alberti, S., and Carra, S. (2017) Aberrant Compartment Formation by HSPB2 Mislocalizes Lamin A and Compromises Nuclear Integrity and Function. *Cell Rep* **20**, 2100-2115
29. Malinovska, L., Kroschwald, S., and Alberti, S. (2013) Protein disorder, prion propensities, and self-organizing macromolecular collectives. *Biochim Biophys Acta* **1834**, 918-931
30. Vos, M. J., Kanon, B., and Kampinga, H. H. (2009) HSPB7 is a SC35 speckle resident small heat shock protein. *Biochim Biophys Acta* **1793**, 1343-1353
31. Kaganovich, D., Kopito, R., and Frydman, J. (2008) Misfolded proteins partition between two distinct quality control compartments. *Nature* **454**, 1088-1095
32. Rothe, S., Prakash, A., and Tyedmers, J. (2018) The Insoluble Protein Deposit (IPOD) in Yeast. *Front Mol Neurosci* **11**, 237
33. Muchowski, P. J., and Wacker, J. L. (2005) Modulation of neurodegeneration by molecular chaperones. *Nat Rev Neurosci* **6**, 11-22
34. Bryantsev, A. L., Kurchashova, S. Y., Golyshev, S. A., Polyakov, V. Y., Wunderink, H. F., Kanon, B., Budagova, K. R., Kabakov, A. E., and Kampinga, H. H. (2007) Regulation of stress-induced intracellular sorting and

chaperone function of Hsp27 (HspB1) in mammalian cells. *Biochem J* **407**, 407-417

35. Rogalla, T., Ehrnsperger, M., Preville, X., Kotlyarov, A., Lutsch, G., Ducasse, C., Paul, C., Wieske, M., Arrigo, A. P., Buchner, J., and Gaestel, M. (1999) Regulation of Hsp27 oligomerization, chaperone function, and protective activity against oxidative stress/tumor necrosis factor alpha by phosphorylation. *J Biol Chem* **274**, 18947-18956
36. Hoop, C. L., Lin, H. K., Kar, K., Hou, Z., Poirier, M. A., Wetzel, R., and van der Wel, P. C. (2014) Polyglutamine amyloid core boundaries and flanking domain dynamics in huntingtin fragment fibrils determined by solid-state nuclear magnetic resonance. *Biochemistry* **53**, 6653-6666
37. Dehay, B., and Bertolotti, A. (2006) Critical role of the proline-rich region in Huntingtin for aggregation and cytotoxicity in yeast. *J Biol Chem* **281**, 35608-35615
38. Tam, S., Geller, R., Spiess, C., and Frydman, J. (2006) The chaperonin TRiC controls polyglutamine aggregation and toxicity through subunit-specific interactions. *Nat Cell Biol* **8**, 1155-1162
39. Mittag, T., and Parker, R. (2018) Multiple Modes of Protein-Protein Interactions Promote RNP Granule Assembly. *J Mol Biol* **430**, 4636-4649
40. Darling, A. L., Liu, Y., Oldfield, C. J., and Uversky, V. N. (2018) Intrinsically Disordered Proteome of Human Membrane-Less Organelles. *Proteomics* **18**, e1700193
41. Robertson, A. L., Headey, S. J., Saunders, H. M., Ecroyd, H., Scanlon, M. J., Carver, J. A., and Bottomley, S. P. (2010) Small heat-shock proteins interact with a flanking domain to suppress polyglutamine aggregation. *Proc Natl Acad Sci U S A* **107**, 10424-10429
42. Cohen, S. I., Vendruscolo, M., Dobson, C. M., and Knowles, T. P. (2012) From macroscopic measurements to microscopic mechanisms of protein aggregation. *J Mol Biol* **421**, 160-171
43. Monsellier, E., Redeker, V., Ruiz-Arlandis, G., Bousset, L., and Melki, R. (2015) Molecular interaction between the chaperone Hsc70 and the N-terminal flank of huntingtin exon 1 modulates aggregation. *J Biol Chem* **290**, 2560-2576

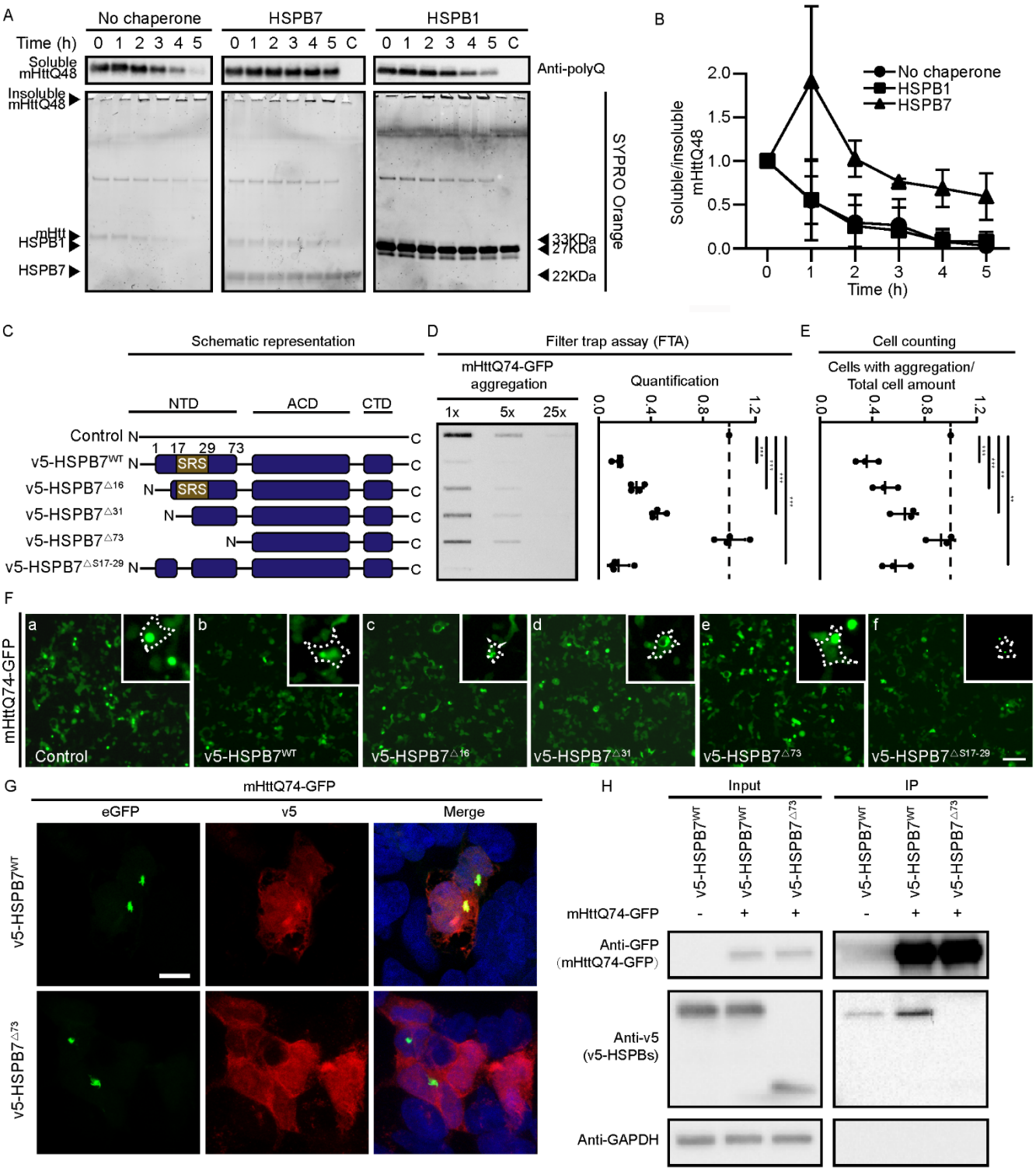

Figure 1. Direct interaction with and prevention of polyQ protein aggregation by HSPB7 is dependent on its full NTD. **A-B**, HSPB7 prevents mHttQ48 aggregation *in vitro*. A purified exon-1 fragment of Huntingtin (mHttQ48) was incubated without chaperones or with either HSPB7 or HSPB1 for 0-5 hours at 37 °C and processed on SDS-PAA gels. **A**, Soluble mHttQ48 was detected by western blot using anti-polyQ antibody (upper row). Soluble and insoluble mHttQ48 as well as HSPBs levels were also detected by SYPRO orange staining of the SDS-PAA gels (lower row). "C" means control in which HSPB1 or HSPB7 were incubated at 37 °C for 5 h without mHttQ48. **B**, Quantification of the ratio of soluble to insoluble mHttQ48. **C**, Schematic representation of HSPB7 NTD truncated mutants. **D**, Filter trap assay (FTA) of the effects of HSPB7^{WT} or NTD truncated mutants on polyQ (mtHttQ74) aggregation in HEK293 cells (left). Control samples were transfected with mRFP. Quantifications are shown on the right, normalized to control (= 1.0). **E**, Quantification of cells displaying mHttQ74-

GFP aggregates when expressed together with mRFP (control =1.0), $HSPB7^{WT}$ or its mutants. **F**, Representative immunofluorescence pictures of HEK293 cells expressing mHttQ74-GFP with control plasmid (mRFP) or together with $HSPB7^{WT}$ or its mutants (bar=100 µm, zoom in upper right, dotted lines indicate the cell outlines). **G**, Immunofluorescence staining of HEK293 cells co-expressing mHttQ74-GFP (green) with v5-$HSPB7^{WT}$ (upper row in red) or v5-$HSPB7^{\Delta 73}$ (lower row in red). Bar = 10 µm. **H**, Co-immunoprecipitation of $HSPB7^{WT}$ but not $HSPB7^{\Delta 73}$ with mHttQ74-GFP. Western blot with the indicated antibodies is shown. All experiments were repeated at least three times. Data are presented as mean ± SD. " * " = $P<0.05$, " ** " = $P<0.01$.

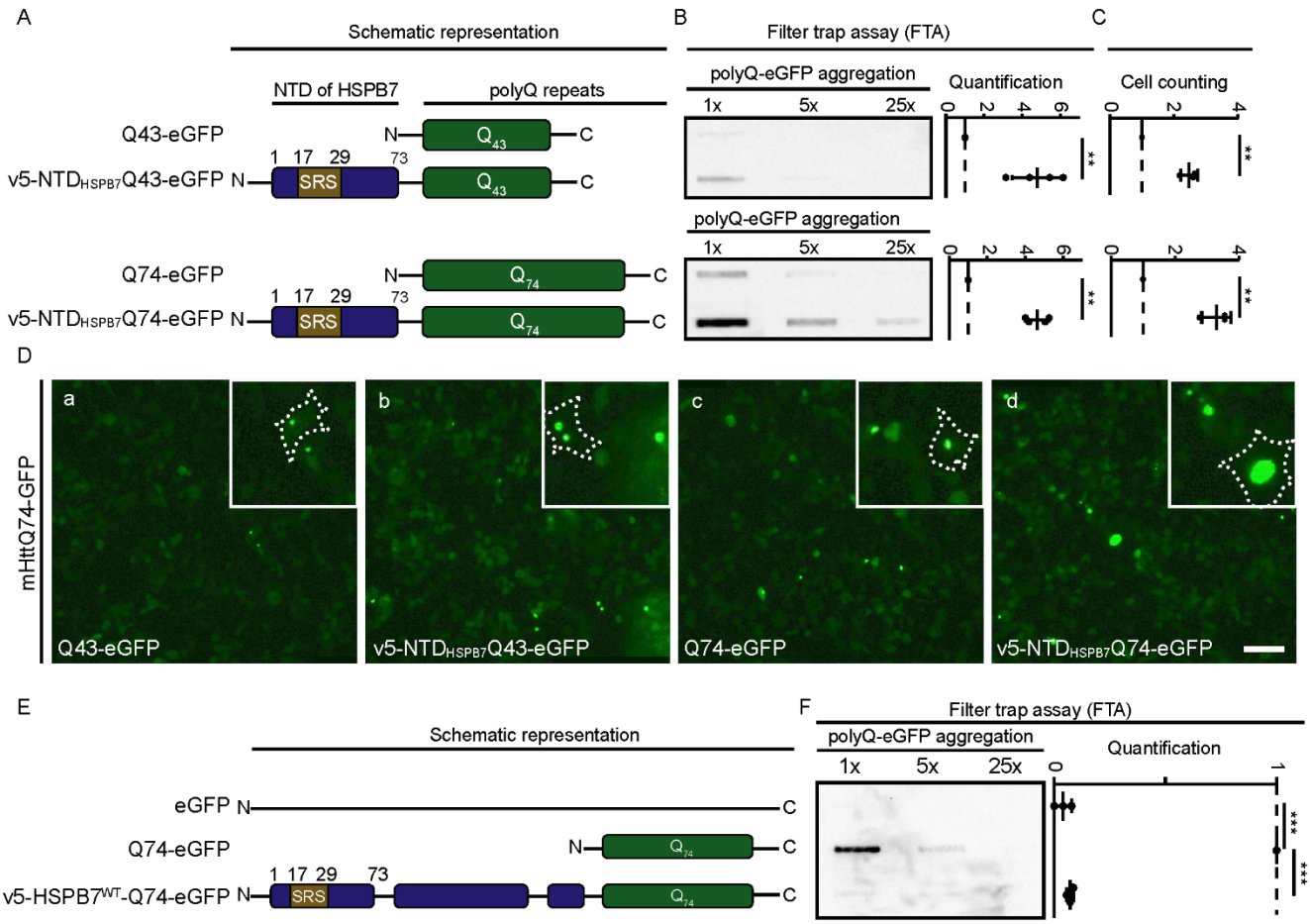

Figure 2. The NTD of HSPB7 alone is not sufficient to prevent polyQ aggregation.
A-D, Fusing the NTD of HSPB7 to mHttQ74-GFP does not prevent polyQ aggregation. **A,** Schematic representation of the different chimeric proteins. **B**, Filter trap assay (FTA) of v5-NTD$_{HSPB7}$Q43-eGFP and v5-NTD$_{HSPB7}$Q74-eGFP expressing HEK293 cells (left). Quantification of polyQ aggregation measured by FTA normalized to the control (Q43-eGFP or Q74-eGFP respectively = 1.0) (right) . **C-D,** PolyQ inclusions in cells expressing v5-NTD$_{HSPB7}$Q43-eGFP and v5-NTD$_{HSPB7}$Q74-eGFP. **C,** Quantification of cells with aggregates, corrected for the total number of cells and normalized to control (Q43-eGFP or Q74-eGFP respectively = 1.0). **D,** Representative immunofluorescence pictures of HEK293 cells expressing different chimeric proteins (bar = 100 µm, zoom in upper right, dotted lines indicate cell outlines). **E-F**, Fusing full length HSPB7 to mHttQ74-GFP prevents polyQ aggregation. **E,** Schematic representation of the chimeric proteins. **F,** FTA of v5-HSPB7^{WT}-Q74-eGFP expressing HEK293 cells. (left) and quantification of polyQ aggregation measured by FTA normalized to the control (Q74-eGFP alone)(right). All experiments were repeated at least three times. Data are presented as mean ± SD. " * " = P<0.05, " ** " = P<0.01.

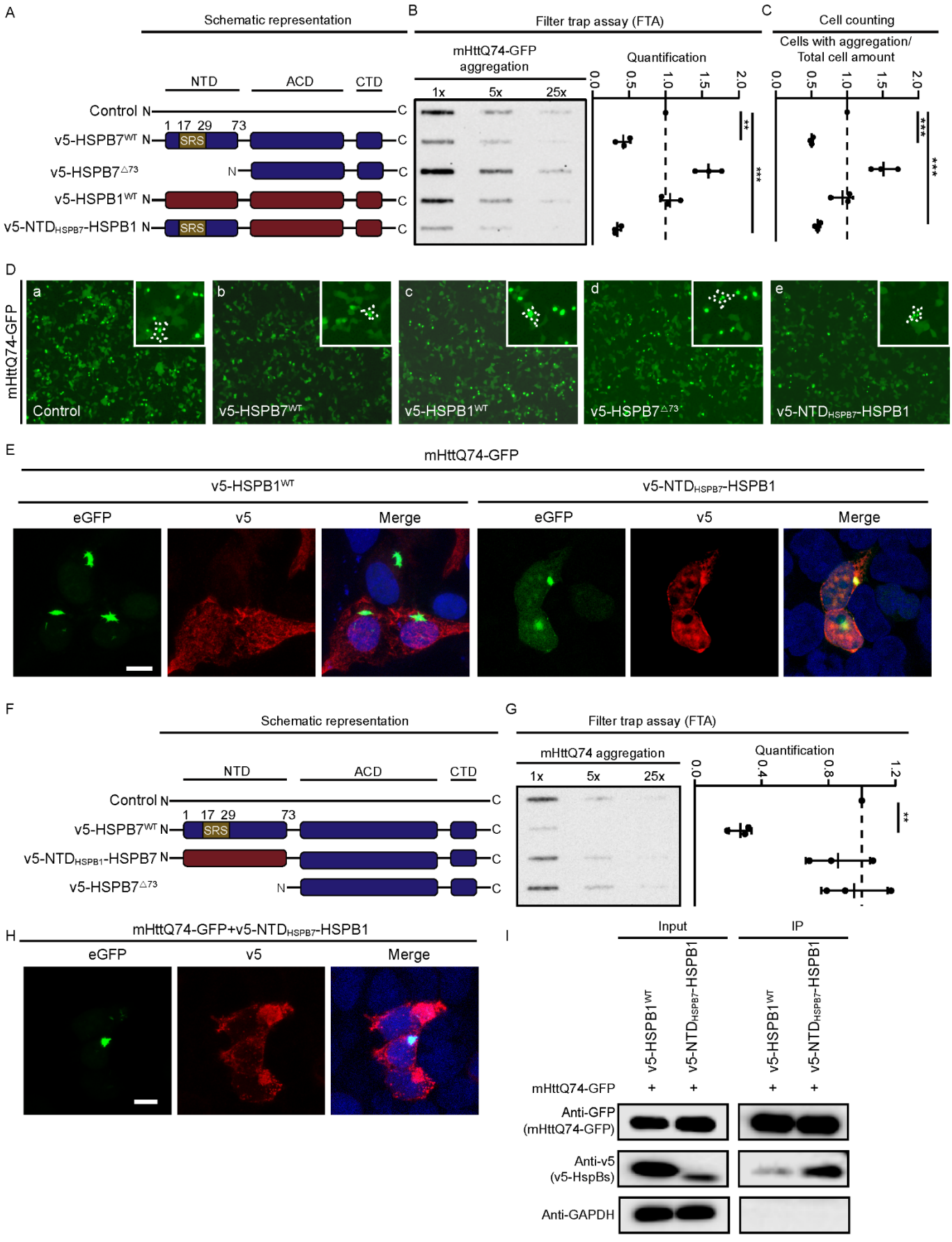
A
Schematic representation
NTD
ACD
CTD
Control
v5-HSPB7WT
v5-HSPB7△73
v5-HSPB1WT
v5-NTDHSPB7-HSPB1
SRS
B
Filter trap assay (FTA)
mHttQ74-GFP aggregation
1x
5x
25x
Quantification
C
Cell counting
Cells with aggregation/ Total cell amount
D
mHttQ74-GFP
Control
v5-HSPB7WT
v5-HSPB1WT
v5-HSPB7△73
v5-NTDHSPB7-HSPB1
E
mHttQ74-GFP
v5-HSPB1WT
v5-NTDHSPB7-HSPB1
eGFP
v5
Merge
F
Schematic representation
G
Filter trap assay (FTA)
mHttQ74 aggregation
Quantification
H
mHttQ74-GFP+v5-NTDHSPB7-HSPB1
I
Input
IP
mHttQ74-GFP
Anti-GFP (mHttQ74-GFP)
Anti-v5 (v5-HspBs)
Anti-GAPDH

Figure 3. NTD swapping between HSPB1 and HSPB7 reveals a key role of the NTD of HSPB7 in the prevention of polyQ aggregation.

A, Schematic representation of the different chimeric proteins. **B**, Filter trap assay (FTA) of the effect of the indicated HSPB variants on mHttQ74-GFP aggregation in HEK293 cells (left). As a control cells were transfected with mRFP. Quantification of mHttQ74-GFP aggregation is normalized to control (= 1.0) (right). **C-D**, mHttQ74-GFP inclusions in cells which co-express the indicated HSPB variants. **C**, Quantification of cells with aggregates per total number of cells, normalized to control (=1.0). **D**, Representative immunofluorescence pictures of HEK293 cells expressing the indicated HSPB variants (bar = 100 µm, zoom in upper right, cell outlines indicated by dotted lines). **E**, Immunofluorescence staining of HEK293 cells co-expressing mHttQ74-GFP (green) and v5-NTD_{HSPB7}-HSPB1 mutant (red) or v5-$HSPB1^{WT}$ (red). Bar = 10 µm. **F**, Schematic representation of the different chimeric proteins. **G,** Filter trap assay (FTA) of the effect of the indicated HSPB variants on mHttQ74-GFP aggregation in HEK293 cells (left). As a control cells were transfected with mRFP. Quantification of mHttQ74-GFP aggregation is normalized by control (-1.0) (right). **H**, Immunofluorescence staining of HEK293 cells showing no colocalization of mHttQ74-GFP (green) with v5-NTD_{HSPB1}-HSPB7 mutant (red). Bar = 10 µm. **I**, Co-immunoprecipitation of v5-NTD_{HSPB7}-HSPB1 but not $HSPB1^{WT}$ with mHttQ74-GFP but $HSPB1^{WT}$. Western blot using the indicated antibidies are shown. All experiments were repeated for at least three times. All experiments were repeated at least three times. Data are presented as mean ± SD. " * " = $P<0.05$, " ** " = $P<0.01$.

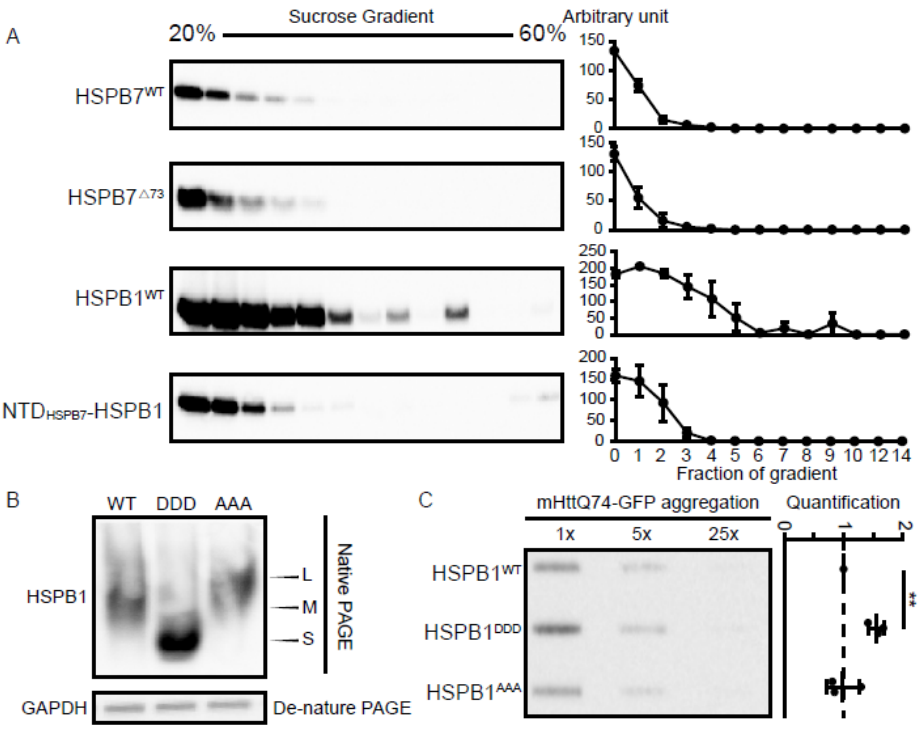

Figure 4. The relation between the oligomeric status of HSPB variants and their abilities to prevent polyQ aggregation. **A**, Sucrose gradient centrifugation analysis of HSPB variants expressed in HEK293 cell in a linear 20 – 60% sucrose density gradient. Representative immunoblots are presented on the left, quantitative analysis are shown on the right. **B**, Native gel electropheresis of HEK293 cells expressing $HSPB1^{WT}$ (WT), $HSPB1^{DDD}$ (DDD), or $HSPB1^{AAA}$ (AAA). Arrows show oligomeric size as large (L), medium (M) and small (S) size. GAPDH was detected by denaturing PAGE as reference. **C**, Filter trap assay (FTA) of $HSPB1^{DDD}$ and $HSPB1^{AAA}$ mutants on mHttQ74-GFP aggregation in HEK293 cells (left). Quantification of polyQ aggregation are normalized by control (=1.) and are shown on the right. All experiments were repeated at least three times. Data are presented as mean ± SD. " ** " = P<0.01.

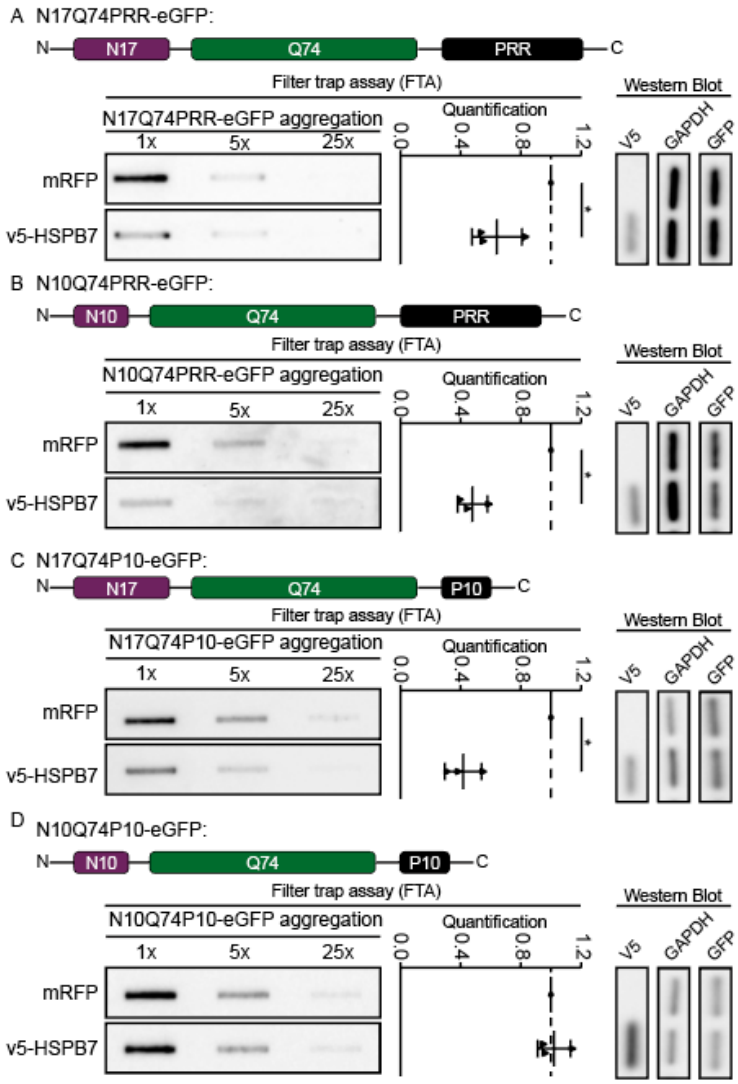

Figure 5. HSPB7 prevents mHtt aggregation via interactions with the polyQ flanking regions.
A-D. Schematic representation of the constructs of different mHtt mutants are presented on the top (N17 = intact NTD; N10 = disturbed NTD; PRR = intact proline rich region; P10 is disturbed proline rich region. Representative immunoblots of FTA (left panels) and quantifications (middle panels) and expression levels of different mHtt and v5-HSPB7 constructs as detected by western blot (right panel) are presented. All quantifications are normalized to cells transfected with mHttQ74-GFP mutants and mRFP (=1.0). All experiments were repeated at least three times. Data are presented as mean ± SD. " * " stands for $P<0.05$.